Computational model for multiple acoustic levitation points with an ultrasonic plane wave and a grid of reflecting surfaces

Spyros Polychronopoulos
Current affiliation: Informatics and Telecommunications Department, National and Kapodistrian University of Athens, Zografou 161 22, Athens, Greece
This work's affiliation: Informatics Department, University of Sussex, Falmer, Brighton, BN1 9QJ, UK

ABSTRACT

Since the first levitation of an object with sound, almost a century ago, acoustic levitation is still a rather active field of research; mainly because there are no constraints regarding the levitated object's material and because of the manipulation precision. These two aspects are enabling several applications both for lab experiments and for human-computer interaction apparatus. The two broadly used techniques involve standing waves and focusing the acoustic energy in specific locations, with one or more arrays of phased ultrasonic transducers. However, by putting the first one into practice the levitation points are in predefined positions and with the second one each acoustic trap is getting weaker as a new one is being introduced. Here we introduce a method combining the above techniques by adopting one transducer or a single phased array and a grid of reflecting surfaces with various heights. Our method is using numerical optimization techniques to optimize the reflecting surfaces' heights to form multiple levitation points at given locations. By combining the emitted with the reflected sound pressures the acoustic field gets stronger and more capable of levitating multiple objects.

Υπολογιστικό μοντέλο για ακουστική αιώρηση πολλαπλών σωμάτων με υπερήχους και συστοιχία ανακλαστικών επιφανειών

ΠΕΡΙΛΗΨΗ

Από την πρώτη αιώρηση ενός αντικειμένου με ήχο, σχεδόν πριν από έναν αιώνα, η ακουστική αιώρηση εξακολουθεί να είναι ένα αρκετά ενεργό πεδίο έρευνας κυρίως επειδή δεν υπάρχουν περιορισμοί σχετικά με το υλικό του ανυψούμενου αντικειμένου και λόγω της ακρίβειας χειρισμού. Αυτές οι δύο πτυχές επιτρέπουν πολλές εφαρμογές τόσο για εργαστηριακά πειράματα όσο και για συσκευές αλληλεπίδρασης ανθρώπου-μηχανής. Οι δύο ευρέως διαδεδομένες τεχνικές περιλαμβάνουν στάσιμα κύματα και εστίαση της ακουστικής ενέργειας σε συγκεκριμένα σημεία, με μία ή περισσότερες

συστοιχίες από ηχεία υπερήχων που έχουν τη δυνατότητα να έχουν διαφορετική φάση το καθένα. Ωστόσο, με την εφαρμογή της πρώτης, τα σημεία αιώρησης βρίσκονται σε προκαθορισμένες θέσεις και με τη δεύτερη ακουστική ενέργεια του κάθε σημείου αιώρησης εξασθενεί όταν εισάγεται ένα νέο σημείο. Εδώ εισάγουμε μια μέθοδο που συνδυάζει τις παραπάνω τεχνικές υιοθετώντας μια μονοφασική συστοιχία ηχείων υπερήχων και μια συστοιχία ανακλαστικών επιφανειών με διάφορα ύψη. Η μέθοδός μας χρησιμοποιεί τεχνικές αριθμητικής βελτιστοποίησης για τη βελτιστοποίηση των υψών των ανακλώμενων επιφανειών ώστε να σχηματίζονται πολλαπλά σημεία αιώρησης σε δεδομένες θέσεις. Συνδυάζοντας τις εκπεμπόμενες με τις ανακλώμενες ηχητικές πιέσεις, το ακουστικό πεδίο γίνεται ισχυρότερο και πιο ικανό να για αιώρηση πολλαπλών αντικειμένων.

Introduction

The physics behind levitating and manipulating objects with acoustic waves has been explicitly explored[1–5] providing us with a satisfactory understanding of the phenomenon. Innovative applied works reveal new areas suitable for utilization; In biology, by the manipulation of yeast cells[6], levitating small living animals[7], using levitated drops for biophysical measurements[8], sample delivery[9] and cell manipulation[10]. In chemistry, by levitating liquids[11], for chemical analysis[12,13] and mixing in colliding levitated drops[14] and in gastronomy[15]. In human computer interaction; food delivery[16], visualization[17,18] and interactive widgets[19]. Additionally, for wearable levitators incorporation of an electrostatic field can allow rotation of the levitated objects, producing mid-air displays[20]. A magnetic field can also be employed to wirelessly charge the levitated object, such as a light-emitting moving particle[21].

The transducer-opposing reflector setup or transducer-opposing transducer setup, to obtain more stable traps, was one of the first methods to levitate objects with ultrasound[22–24]. However, it is still commonly used to manipulate, in one direction, one or more objects[25–29]. This approach is based on the creation of a standing wave where the nodes act as traps. Moreover, by either changing the transducers' phases[30,31] or by changing their amplitudes[25] the nodes, and therefore the levitated objects, move in a single axis. By amending both transducers' phases and amplitudes one or more objects can be manipulated in 3D[32]. However, until now, there is not extensive research for the same set of transducers to control more than one trap. The objects, implementing the standing wave method, can levitate at set distances of half a wavelength ($\lambda/2$) between them and by changing the phase of the transducers they can move altogether to the same direction at the same speed[20].

Two new methods made the levitation of an object larger than the wavelength possible. The first method brought about the levitation of a polystyrene bead approximately 2λ in diameter, in an acoustic trap, by exploring the angular momentum that acoustic vortices can transfer[33] The second method involves creating a standing wave between the transducer and object. By implementing the

second method scientists managed to levitate in the near-field large sized planar objects[34,35]. Although the wavelength limit, regarding the size of the levitated object, was broken, the original constrain of one individual trap per set of transducers, until now, remains. This is setting a barrier and not allowing the development of more innovative applications. In addition, the stability of the levitated object is always an issue[36].

With the use of pre-manufactured, three-dimensional units (so called acoustic metamaterials), controlling the sound-field can be done with greater efficiency[37] and even enable the representation of shapes in 2D[38]. The aforementioned metamaterials are introducing specific phase delays on the acoustic wave and act as lenses that can focus or steer the wave. Our approach is also based on the phase delays that acoustic elements are introducing. However, the proposed reflecting grid of surfaces is adopting the acoustic energy coming from the reflections to create more stable and independent traps in selected positions.

Currently, the dominant method to create more than one independent trap at certain locations incorporates a phased array of transducers, where each set of transducers is responsible for one trap[39]. Nonetheless, a phased array requires the individual control of each transducer which requires elaborate and pricy electronics. Further, every new trap will weaken the strength and stability of the entire group of traps, as less transducers will contribute per trap. This seriously limits the maximum number of stable traps per array.

In the microworld an electronically controlled acoustic tweezer was used to demonstrate multiple Bessel function shaped traps by calculating the applied signals for each desired trap accordingly and then performing a linear superposition[40]. The acoustic tweezers consist of a circular 64-element ultrasonic array operating in the MHz region and they can manipulate polystyrene spheres in the μm region in diameter. However, this method can only be applied in small wavelengths signals and therefore manipulate small objects.

Here we propose a setup that maximizes the traps' strength, for an ultrasound field of any frequency, by adopting a grid of reflecting surfaces that is able to manipulate the generated pressure and shape the sound-field in order to create multiple levitation points. Adopting this method means that the transducers do not need to be connected to complicated electronics driving their phases and amplitudes as they only need to be in phase and emit, for better results, in their maximum power.

The computational method and the algorithm for the setup are described in detail. The first step is to introduce the physical parameters of the transducers, the reflecting grid and the positions of the levitated objects. From here the algorithm uses heuristic optimisation technique to calculate the optimal displacements for the grid of reflectors to be installed opposite the transducer or the array of transducers. Our goal is to shape the pressure field around certain points and create acoustic traps. The only functionable variables in this apparatus are the vertical displacements of the grid's reflectors. This is a nonlinear problem that requires global optimization. For nonlinear problems where finding an approximation of the global optimum is more important than finding a more precise local optimum, simulated annealing (SA) optimizer is preferable to alternatives, such as gradient descent. Thus, our algorithm is incorporating SA as it is a more suitable optimizer for our problem.

1. Method

An algorithm that calculates the optimized set of displacements for a grid of reflectors per input set of parameters is coded in Rust programming language. The output displacements are introduced in a MATLAB algorithm that simulates the signals and by discretizing the field calculates and plots the pressure field in 3D.

Firstly, the algorithm calculates the pressure at the chosen levitation points, as a factor of reflectors' displacements, z_n. It should be noted here that, for simplification reasons, higher than second order reflections and attenuation due to distance or the reflections, were not considered. The above simplifications can be made and not significantly affect the accuracy of the simulation as we constrain the emission frequency in the ultrasound region, the reflecting surfaces been made from a non-absorptive/porous material and the reference distance from the transducer to the grid to be less than 20λ ($h < 20\lambda$). Further, it is assumed that the levitation points are above 2λ from the transducer (vibrating plate with planar propagation) or the array of single phased transducers. Therefore, the emitted signal can be simulated as a plane propagated signal. The reflectors' were simulated as point sources with emissions' directivity[41], emitting from their image location and utilizing the image source method[42]. Thus, the pressure at any position with (x, y, z) Cartesian coordinates can be calculated by equation (1):

$$p = \underbrace{p_0 e^{ikz}}_{direct\ signal} * \underbrace{p_0 \sum_{n=1}^{N^2} H_{(n)} e^{ikd_{im(n)}}}_{reflection\ signals} \tag{1}$$

Where p_0 is the transducer's reference pressure, k is the wavenumber $k = \frac{2\pi}{\lambda}$, * denotes the convolution, N^2 is the total number of reflecting surfaces, d_{im} is the distance from the image reflectors' positions to the traps' positions. The reflecting surfaces' directivity H is calculated by[41]:

$$H_{(n)} = \left| sinc\left(\frac{\pi a}{\lambda} sin\,\theta_{(n)}\, cos\,\varphi_{(n)}\right) sinc\left(\frac{\pi b}{\lambda} sin\,\theta_{(n)}\, sin\,\varphi_{(n)}\right)\right| \tag{2}$$

Where: a, b are the reflecting surfaces dimensions, θ the azimuthal angle $\theta_{(n)} = \arccos\left(\frac{z-(h-z_{(n)})}{d_{re(n)}}\right)$ and φ the elevational angle $\varphi_{(n)} = \arctan\left(\frac{y-y_{(n)}}{z-x_{(n)}}\right)$, as shown in Figure 1. For d_{re} being the distance from the real reflectors' positions to the traps' positions.

Then the Gorkov's potential is calculated by equation[2] (3):

$$U = k_1|p^2| - k_2\left(|p_x|^2 + |p_y|^2 + |p_z|^2\right) \tag{3}$$

Where,

$k_1 = \frac{2\pi}{3} a_T^3 \kappa_0 (1-\tilde{\kappa})$, $k_2 = a_T^3 \pi \rho_0 \frac{2(\tilde{\rho}-1)}{2\tilde{\rho}+1}$, a_T is the trap's radius, $\tilde{\kappa} = \frac{\kappa_p}{\kappa_0}$, with κ_p and κ_0 being the object's and the medium's compressibility factors, respectively and

$\tilde{\rho} = \frac{\rho_p}{\rho_0}$, with ρ_p and ρ_0 being the object's and the medium's densities, respectively and p_x, p_y and p_z are the first order derivatives of the pressure over x, y and z coordinates.

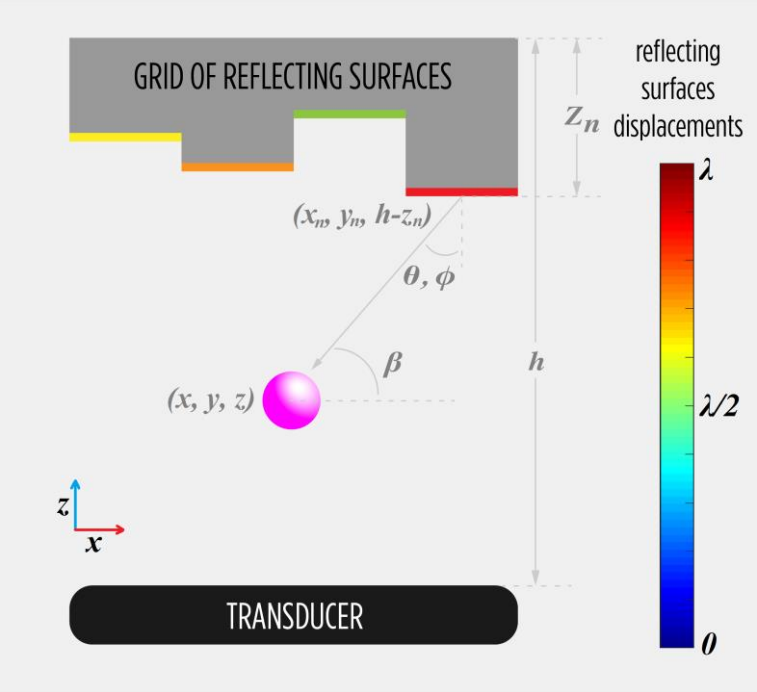

Figure 1. 2D representation of the proposed model showing a. the angles to calculate both the reflectors' directivity and their weighting, the reference distance between the transducer and the reflectors' and the grid's height displacements b. the transducer, the grid of reflecting surface and the sound waves.

1.1 Optimizer

We define a levitation point by constraining the summation of the absolute value of the pressure with the negative Laplacian of the Gorkov's potential at this point to be less than K. Assuming that the trap's diameter is significantly smaller than the sound-field's wavelength[2], the value of K is dependant only on the levitated particles' and the medium's density. In this work we show computational results for the levitation of polystyrene beads in the air and therefore the factor K needs to be less than 400.

The brute-force calculation of the optimum reflectors' heights in order to create one or more acoustic traps is not computationally possible as there are an extensive number of permutations. As an example, even a small grid of 4×4 reflectors and only 5 height displacement steps (z_n) per reflector, the number of permutations is around 10^{11}.

The method used to obtain the optimal reflectors' displacements in order to create acoustic traps at given locations is a SA algorithm[43]. SA is a nonlinear optimizer that

can approximate the global minimum of a given function, commonly known as the objective function. The simulation of annealing can be either executed by a solution of kinetic equations for density functions[44] or by using the stochastic sampling method[45]. The method used here is an adaptation of the Metropolis–Hastings algorithm, a Monte Carlo method to generate sample states of a thermodynamic system[46]. It is less computationally expensive to minimize a function rather than maximizing it; therefore, we minimize the negative function $-f$ instead of maximizing the function f. In order to minimize the pressure, maximize the Laplacian of the Gorkov's potential and to ensure that the solution fulfils the levitation requirement for every selected position, the objective function formed is:

$$O_{(z_n)} = \sum_{m=1}^{M} \left(\left| p_{m(z_n)} \right| - \Delta U_{m(z_n)} + Q_{m(z_n)} \right) \tag{4}$$

Where M is the number of traps, $\Delta U = U_{xx} + U_{yy} + U_{zz}$ is the Laplacian of the Gorkov's potential, with U_{xx}, U_{yy} and U_{zz} being the second order derivatives of the Gorkov's potential over x, y and z coordinates, Q is a function that equals zero when the requirement for levitation is fulfilled otherwise equals a large number (L).

$$Q_{m(z_n)} = \begin{cases} 0, \text{for } \left| p_{m(z_n)} \right| - \Delta U_{m(z_n)} < K \\ L, \text{for } \left| p_{m(z_n)} \right| - \Delta U_{m(z_n)} \geq K \end{cases}$$

By adding Q function in equation (4), when the levitation requirement is not fulfilled the SA will look for another set of values as the objective function is not minimized.

1.2 Weighting

In order to optimize the random reflectors' displacement values (z_n) that SA generates at every iteration and more efficiently track down the optimum set of candidates, we applied a weighting factor to each reflecting surface. The algorithm considering the effectiveness of each reflector to each trap and then averaging the results:

$$W = \frac{1}{M} \sum_{m=1}^{M} W_m \tag{5}$$

Where,

$$W_m = \begin{bmatrix} \widehat{\sin \beta_{m(1,1)}} & \cdots & \widehat{\sin \beta_{m(1,N)}} \\ \vdots & \ddots & \vdots \\ \widehat{\sin \beta_{m(N,1)}} & \cdots & \widehat{\sin \beta_{m(N,N)}} \end{bmatrix}$$

for $N \times N$ reflecting surfaces, $\sin \beta_{m(n)} = \frac{(h+z_n)-z_m}{d_n}$ and the accent $\widehat{\ }$ denotes the normalization. The weighting representation example for a grid of 16×16 reflecting surfaces with one and two traps in the middle and in symmetrical opposing positions from the middle of the grid, respectively, is shown in Figure 2.

The weighting, equation (5), is considered in order to optimize the generation of the random displacement values (z_d) at every iteration of SA. The weighting factor denotes the likelihood to change the previous randomly generated displacement

value of each reflector, at every new iteration, and create a new set of random values.

The matrix R^q with N^2 randomly generated set of values, one for each z_d reflector's displacement, from 0 to λ is coded as shown in coding formula (6).

$$R^q = \underbrace{\left[\frac{R_\lambda + R_\lambda E_W}{2R_\lambda}\right] R_\lambda}_{\text{generate new set of values}} + \underbrace{\left[J - \frac{R_\lambda + R_\lambda E_W}{2R_\lambda}\right] R^{q-1}}_{\text{keep the previous set of values}} \quad (6)$$

Where, q is the current iteration, R_λ is a matrix of N^2 random elements from 0 to λ, J is a N^2 elements matrix of ones, R^0 (at the first iteration) would be the training values which are small random numbers, $E_w = \frac{\frac{R_1}{W} - \frac{R_1}{1-W} + \gamma}{\left|\frac{R_1}{W} - \frac{R_1}{1-W} + \gamma\right|}$, for R_1 been a matrix of N^2 random elements from 0 to 1 and γ is a small constant value that ensures that the result will not be zero. The proposed model with the levitated objects creating a smiley face is shown in Figure 3.

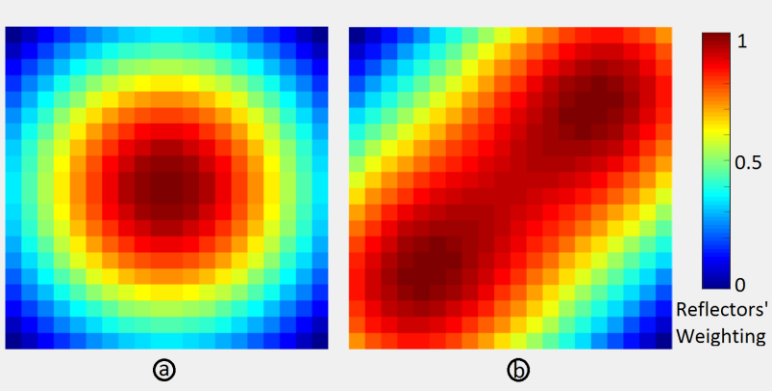

*Figure 2. Weighting representation example for a grid of 16*16 reflecting surfaces with a. one and b. two traps, in the middle and in symmetrical opposing positions from the middle of the grid, respectively.*

1.3 Operation

After setting the traps locations, the number, the reference height (h) and the dimensions of the grid's reflectors, the transducer's max emission pressure and frequency, the algorithm calculates the optimum displacements for the grid's reflecting surfaces. For the grid to be more effective, and also comply with the limitation raised in the method section, it should not be far from the transducer (<20λ). It should be noted here that according to the Nyquist theorem, reconstructing a sound field of a specific frequency without artefacts will require the sound sources (in the proposed setup the reflecting surfaces) to be placed at a distance of less than half of the wavelength (λ/2). Therefore, the maximum proposed dimensions for the reflectors would be $\lambda/2 \times \lambda/2$.

2. Results and discussion

This and the standing wave levitation methods are both limited; vertical distances between the traps must be a multiple of half of a wavelength ($\lambda/2$). However, the advantage of our method is that in a horizontal distance of larger than 5λ the set of vertical positions can be shifted up or down. In Figure 3 three different horizontal distances between the levitation points are shown as the vertical distance between the two points is set to 1mm. The distances between the levitation points are 5λ, 4λ and 3λ in Figures 3a, 3b and 3c, respectively. As the two levitation points are getting closer the required pressure fields, one for each trap, interfere and cancelling both levitation points.

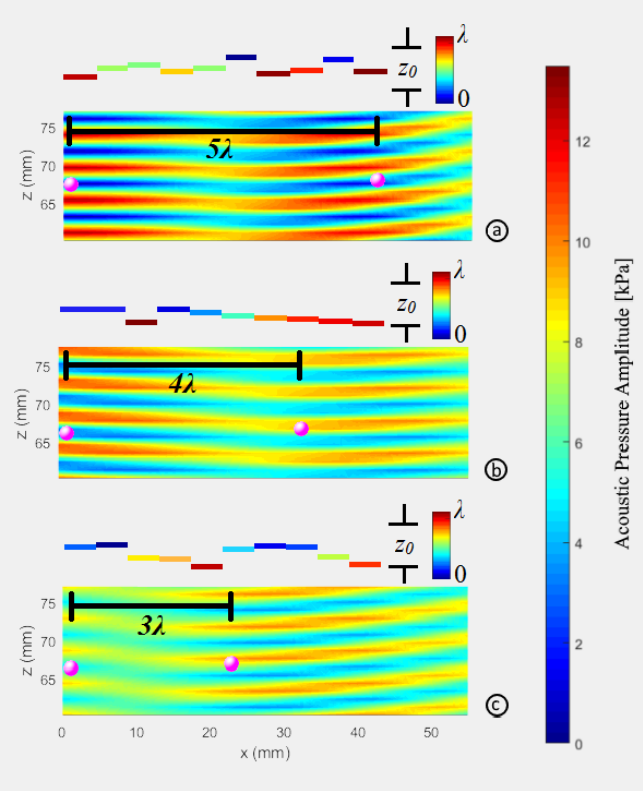

Figure 3. Pressure field and reflectors' displacements (z0) in a section of two traps with vertical distance 1mm and horizontal distance a. 5λ b. 4λ c.5λ. The interference between the two required pressure fields gets stronger as the levitation points get closer and cancelling each other out.

For the example shown here we used transducer's signal of 40kHz and the reflectors dimensions were set to $a = b \approx 4.3\text{mm}$. The reference distance from the transducer to the grid was set to $h = 20\lambda \approx 171.5\text{mm}$, the medium was set to air

and the levitated object was set to polystyrene sphere of 2mm in diameter. The number of traps was set to 8 forming a smiley face as shown in Figure 4. The number of reflecting surfaces was set to N^2=400 (an array of 20×20 reflectors), and the reference transducer pressure to $p_0 = 6$kPa. The number of traps, as well as the number of reflecting surfaces, play a significant role in the run-time of the algorithm. For example for a grid of N^2=400 reflectors if there is a satisfactory solution ($\sum_{m=1}^{M} Q_{m(z_n)} < K$) every new trap will delay the algorithm's run time approximately 4mins. SA's start temperature was set to 1000, the end temperature to 5 and the cooling down temperature step to 0.9999 and the number of iterations for the above set of parameters was 50,000.

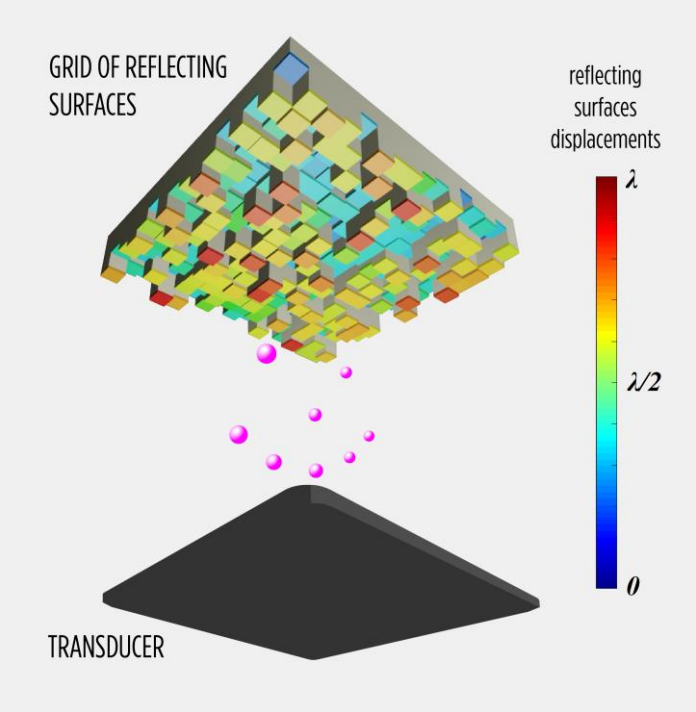

Figure 4. 3D representation of the proposed model showing the transducer, the grid of 16x16 reflecting surfaces with various height displacements to create the acoustic traps in specific positions forming a smile with levitated polystyrene beads.

The algorithm run on a computer with Windows 10 operating system, an AMD Ryzen 7 1700 eight core processor of 3GHz and 16GB of RAM. The SA optimizer implemented in Rust run 50,000 iterations in approximately 30mins for a 20×20 grid of reflectors and 8 traps. The pressure field shown in Figures 3 and 5 is calculated with a MATLAB algorithm by calculating the absolute value of the pressure $|p|$, as described in equation (1), in a 3D discretized field with a λ/8 discretization step. The relative pressure field in 3D is shown in Figure 5.

We here present an objective function, equation (4), that that can be introduced to any optimisation algorithm and find the optimal displacement values for a grid of reflectors, opposing a transducer, and create multiple independent acoustic traps in

the sound field. The objective function is formed in such a way in order to minimize the pressure, maximize the Laplacian of the Gorkov's potential and to ensure that the solution fulfils the levitation requirement for every selected position. Further, we optimize the random set of values the algorithm generates at each iteration. By taking into account the chosen levitation points we calculate the contribution of each reflecting surface in the creation of this set of traps and apply a weighting factor, equation (5). At each iteration the likelihood for the algorithm to generate a new displacement value for each reflector depends on its weighting, equation (6).

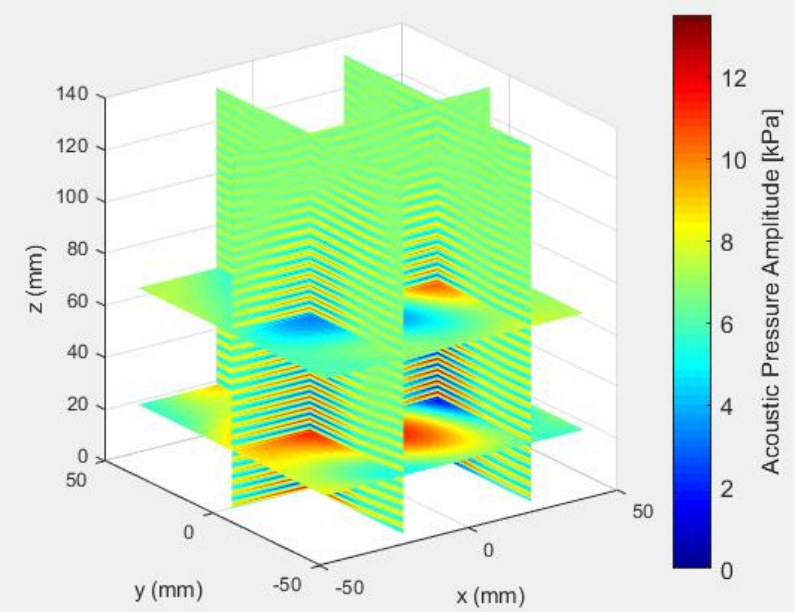

Figure 5. *3D representation of the pressure field and two traps located in x_1=26, y_1=0, z_1=23mm and x_2=-17, y_2=0, z2=68mm*

3. Conclusion

Our proposed method, of a transducer and an opposing grid of reflectors with variable heights, is enabling the shaping of a strong pressure field and the creation of multiple independent levitation points. A static arrangement of levitated objects with only one transducer or an array of single phased transducers now becomes feasible by simply calculating the relevant reflectors' height displacements, 3D printing the reflectors' grid and installing it opposite the transducer(s). With our method there is no need for expensive and complicated electronics driving the transducers' phases and amplitudes to effectively shape the sound field for multiple levitation points.

Although we cannot calculate the reflectors' heights in real time at this point, we could predetermine various arrangements with levitated particles; and by pre-computing the relevant reflectors' heights, a dynamic grid of reflectors would manipulate the levitated objects independently in 3D. Therefore, configurations that change their shape over time could be formed bringing about the first acoustic levitation 3D display.

4. References

1. Zhao, S. & Wallaschek, J. A standing wave acoustic levitation system for large planar objects. *Archive of Applied Mechanics* **81**, 123–139 (2011).
2. Bruus, H. Acoustofluidics 7: The acoustic radiation force on small particles. *Lab on a Chip* **12**, 1014 (2012).
3. Xie, W. J. & Wei, B. B. Resonance shift of single-axis acoustic levitation. *Chinese Physics Letters* **24**, 135–138 (2007).
4. Mitri, F. G. Intrinsic acoustical cross sections in the multiple scattering by a pair of rigid cylindrical particles in 2D. *Journal of Physics D: Applied Physics* **50**, (2017).
5. Sommers, B. S. & Foster, J. E. Nonlinear oscillations of gas bubbles submerged in water: Implications for plasma breakdown. *Journal of Physics D: Applied Physics* **45**, (2012).
6. Hawkes, J. J., Cefai, J. J., Barrow, D. A., Coakley, W. T. & Briarty, L. G. Ultrasonic manipulation of particles in microgravity. *Journal of Physics D: Applied Physics* **31**, 1673–1680 (1998).
7. Xie, W. J., Cao, C. D., Lü, Y. J., Hong, Z. Y. & Wei, B. Acoustic method for levitation of small living animals. *Applied Physics Letters* **89**, 1–4 (2006).
8. Scheeline, A. & Behrens, R. L. Potential of levitated drops to serve as microreactors for biophysical measurements. *Biophysical Chemistry* **165–166**, 1–12 (2012).
9. Šrajer, V. & Schmidt, M. Watching proteins function with time-resolved x-ray crystallography. *Journal of Physics D: Applied Physics* vol. 50 Preprint at https://doi.org/10.1088/1361-6463/aa7d32 (2017).
10. Wang, X., Gou, X., Chen, S., Yan, X. & Sun, D. Cell manipulation tool with combined microwell array and optical tweezers for cell isolation and deposition. *Journal of Micromechanics and Microengineering* **23**, (2013).
11. Lü, Y. J., Xie, W. J. & Wei, B. Observation of ice nucleation in acoustically levitated water drops. *Applied Physics Letters* **87**, 1–3 (2005).
12. Tuckermann, R., Puskar, L., Zavabeti, M., Sekine, R. & McNaughton, D. Chemical analysis of acoustically levitated drops by Raman spectroscopy. *Analytical and Bioanalytical Chemistry* **394**, 1433–1441 (2009).
13. Caccamo, M. T., Cannuli, A., Calabrò, E. & Magazù, S. Acoustic Levitator Power Device: Study of Ethylene-Glycol Water Mixtures. *IOP Conference Series: Materials Science and Engineering* **199**, (2017).
14. Chainani, E. T., Choi, W. H., Ngo, K. T. & Scheeline, A. Mixing in colliding, ultrasonically levitated drops. *Analytical Chemistry* **86**, 2229–2237 (2014).
15. Vi, C. T., Ablart, D., Arthur, D. & Obrist, M. Gustatory interface: the challenges of 'how' to stimulate the sense of taste. *Proceedings of the 2nd ACM SIGCHI International Workshop on Multisensory Approaches to Human-Food Interaction* 29–33 (2017).
16. Vi, C. T. *et al.* TastyFloats : A Contactless Food Delivery System. *Proceedings of the 2017 ACM International Conference on Interactive Surfaces and Spaces* 161–170 (2017) doi:10.1145/3132272.3134123.
17. Omirou, T., Marzo, A., Seah, S. A. & Subramanian, S. LeviPath. *Proceedings of the 33rd Annual ACM Conference on Human Factors in Computing Systems - CHI '15* 309–312 (2015) doi:10.1145/2702123.2702333.

18. Norasikin, M. A. *et al.* SoundBender: dynamic acoustic control behind obstacles. in *The 31st Annual ACM Symposium on User Interface Software and Technology* 247–259 (ACM, 2018).
19. Freeman, E., Anderson, R., Andersson, C., Williamson, J. & Brewster, S. Floating Widgets. *Proceedings of the Interactive Surfaces and Spaces on ZZZ - ISS '17* 417–420 (2017) doi:10.1145/3132272.3132294.
20. Sahoo, D. R. *et al.* JOLED: A Mid-air Display based on Electrostatic Rotation of Levitated Janus Objects. *Proceedings of the 29th Annual Symposium on User Interface Software and Technology - UIST '16* 437–448 (2016) doi:10.1145/2984511.2984549.
21. Uno, Y. *et al.* Luciola: A Millimeter-Scale Light-Emitting Particle Moving in Mid-Air Based On Acoustic Levitation and Wireless Powering: A Millimeter-Scale Light-Emitting Particle Moving in Mid-Air Based On Acoustic Levitation and Wireless Powering. *Proc. ACM Interact. Mob. Wearable Ubiquitous Technol. Article* **1**, 1–17 (2017).
22. Brandt, E. H. Levitation in physics. *Science* 349–355 (1989).
23. Matsui, T., Ohdaira, E., Masuzawa, N. & Ide, M. Translation of an object using phase-controlled sound sources in acoustic levitation. *Japanese Journal of Applied Physics* **34**, 2771–2773 (1995).
24. Mitome, H. Ultrasonic levitation and accompanying acoustic streaming. *Japanese Journal of Applied Physics* **28**, 146–148 (1989).
25. Foresti, D., Nabavi, M., Klingauf, M., Ferrari, A. & Poulikakos, D. Acoustophoretic contactless transport and handling of matter in air. *Proceedings of the National Academy of Sciences* **110**, 12549–12554 (2013).
26. Xie, W. J., Cao, C. D., Lü, Y. J., Hong, Z. Y. & Wei, B. Acoustic method for levitation of small living animals. *Appl Phys Lett* **89**, 1–4 (2006).
27. Scheeline, A. & Behrens, R. L. Potential of levitated drops to serve as microreactors for biophysical measurements. *Biophys Chem* **165–166**, 1–12 (2012).
28. Lü, Y. J., Xie, W. J. & Wei, B. Observation of ice nucleation in acoustically levitated water drops. *Appl Phys Lett* **87**, 1–3 (2005).
29. Polychronopoulos, S. & Memoli, G. Acoustic levitation with optimized reflective metamaterials. *Sci Rep* **10**, 1–10 (2020).
30. Freeman, E., Anderson, R., Andersson, C., Williamson, J. & Brewster, S. Floating Widgets. *Proceedings of the Interactive Surfaces and Spaces on ZZZ - ISS '17* 417–420 (2017) doi:10.1145/3132272.3132294.
31. Sahoo, D. R. *et al.* JOLED: A Mid-air Display based on Electrostatic Rotation of Levitated Janus Objects. *Proceedings of the 29th Annual Symposium on User Interface Software and Technology - UIST '16* 437–448 (2016) doi:10.1145/2984511.2984549.
32. Omirou, T., Marzo, A., Seah, S. A. & Subramanian, S. LeviPath. *Proceedings of the 33rd Annual ACM Conference on Human Factors in Computing Systems - CHI '15* 309–312 (2015) doi:10.1145/2702123.2702333.
33. Marzo, A., Caleap, M. & Drinkwater, B. W. Acoustic Virtual Vortices with Tunable Orbital Angular Momentum for Trapping of Mie Particles. *Physical Review Letters* **120**, 044301 (2018).
34. Yano, R., Aoyagi, M., Tamura, H. & Takano, T. Novel transfer method using near-field acoustic levitation and its application. *Japanese Journal of Applied Physics* **50**, 0–5 (2011).

35. Andrade, M. A. B., Okina, F. T. A., Bernassau, A. L. & Adamowski, J. C. Acoustic levitation of an object larger than the acoustic wavelength. *The Journal of the Acoustical Society of America* **141**, 4148–4154 (2017).
36. Andrade, M. A. B., Polychronopoulos, S., Memoli, G. & Marzo, A. Experimental investigation of the particle oscillation instability in a single-axis acoustic levitator. *AIP Adv* **9**, 35020 (2019).
37. Memoli, G. *et al.* Metamaterial bricks and quantization of meta-surfaces. *Nature Communications* **8**, 1–8 (2017).
38. Melde, K., Mark, A. G., Qiu, T. & Fischer, P. Holograms for acoustics. *Nature* **537**, 518–522 (2016).
39. Marzo, A. *et al.* Holographic acoustic elements for manipulation of levitated objects. *Nature Communications* **6**, 1–7 (2015).
40. Courtney, C. R. P. *et al.* Independent trapping and manipulation of microparticles using dexterous acoustic tweezers. *Applied Physics Letters* **104**, 1–5 (2014).
41. Fan, Y., Honarvar, F., Sinclair, A. N. & Jafari, M.-R. Circumferential resonance modes of solid elastic cylinders excited by obliquely incident acoustic waves. *The Journal of the Acoustical Society of America* **113**, 102–113 (2003).
42. Mintzer, D. Transient Sounds in Rooms. *The Journal of the Acoustical Society of America* **21**, 463 (1949).
43. Ingber, L. Simulated annealing: Practice versus theory. *Mathematical and Computer Modelling* **18**, 29–57 (1993).
44. Khachaturyan, A., Semenovsovskaya, S. & Vainshtein, B. The thermodynamic approach to the structure analysis of crystals. *Acta Crystallographica Section A* **37**, 742–754 (1981).
45. Semenovskaya, S. V., Khachaturyan, K. A. & Khachaturyan, A. G. Statistical mechanics approach to the structure determination of a crystal. *Acta Crystallographica Section A* **41**, 268–273 (1985).
46. Metropolis, N., Rosenbluth, A. W., Rosenbluth, M. N., Teller, A. H. & Teller, E. Equation of state calculations by fast computing machines. *Journal Chemical Physics* **21**, 1087–1092 (1953).